JACS
JOURNAL OF THE AMERICAN CHEMICAL SOCIETY
Article
pubs.acs.org/JACS

Interaction of Tricationic Corroles with Single/Double Helix of Homopolymeric Nucleic Acids and DNA

Alessandro D'Urso,[§] Sara Nardis,[‡] Giuseppe Pomarico,[‡] Maria Elena Fragalà,[§] Roberto Paolesse,*[,‡] and Roberto Purrello*[,§]

[§]Department of Chemical Science, University of Catania, Viale A. Doria 6, 95125 Catania, Italy

[‡]Department of Chemical Science and Technologies, University of Rome "Tor Vergata", Via della Ricerca Scientifica 1, 00133 Rome, Italy

Supporting Information

ABSTRACT: In this manuscript a multitechnique approach is proposed to characterize the interaction between new tri-*N*-methylpyridyl corrole (**TMPC**) and its germanium(IV) derivative (**GeTMPC**), with single- and double-stranded nucleic acid homopolymers and calf thymus DNA. The specificity of each spectroscopic technique has been exploited to analyze the different aspects of corrole binding. Noteworthy, this approach allows us to distinguish between H aggregation of **TMPC** in the presence of polyriboadenilic acid (poly(rA)) and J aggregates in the presence of polyribocytidinic acid (poly(rC)) as well as to identify the formation of **GeTMPC** dimers in the presence of single-stranded poly(rA) and pseudointercalation with single-stranded poly(rC).

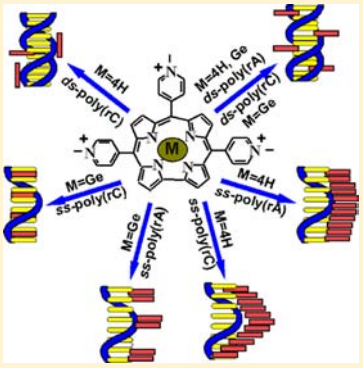

INTRODUCTION

Nucleic acids homopolymers are not simply synthetic model systems since they are also found in nature as stretches of polyriboadenilic acid (poly(rA)) about 200 nucleotides long, covalently linked to the 3′ end of poly disperse nuclear RNA, mRNA of animal cells, and many animal viruses.[1] In eukaryotes, polyadenylation is part of the process that produces mature messenger DNA (mRNA) for translation; the function of the 3′ tail is likely protective, in fact mRNAs without a 3′ tail are rapidly degraded. Polycytidine (C)(n) repeat (poly(rC)) have been found within the D-loop region of the mitochondrial DNA.[2] Somatic mutations at a mitochondrial noncoding polycytidine (C)(n) repeat have been associated with tumor progression.[3]

In general, interactions of small ligands with both single (*ss*) and double stranded (*ds*) nucleic acid polymers has a multifold interest.[4,5] The two most obvious aspects of this research topic are related to the interactions of *ss* and/or *ds* nucleic acids with molecules having antitumoral activity or behaving as possible conformational reporters. It is worth underlying, in fact, that a growing interest is arising on the biological role of nucleic acids conformations.[6]

A very important, and more than promising, class of molecules, which have been successfully employed for both the above-mentioned applications, is that of porphyrins. In fact, in addition to their use as antitumoral drugs, cationic porphyrins can found applications as specific reporters of nucleic acids conformations. Some metallo-derivatives can efficiently distinguish between the B- and the A-forms or can very efficiently detect the left-handed Z-form even when embedded in long B-sequences.[5,7] This characteristic combined with ability to produce single oxygen strongly suggests that porphyrins can be used as structure-selective drugs for photodynamic therapy (PDT).[8]

Distinguishable from porphyrin for the absence of one of the four *meso*-positions, corroles contain three "pyrrole-type" hydrogens (i.e only one protonable nitrogen) in the macrocyclic core together a direct pyrrole−pyrrole link. Corroles are also very promising photosensitizers for PDT therapy and have been found useful to control tumor progression and metastasis in animal models.[9]

In spite of this, only few data are present in literature reporting the interaction of cationic corroles with *ss* and *ds* nucleic acids.[10b,c] As a matter of fact, only sparse reports about corroles with positively charged substituents have been published.[10] These substituents, indeed, are the first choice to study interactions with DNA owing to the expected electrostatic attraction with the negatively charged arrays of phosphate backbone, even if also interactions between anionic porphyrins and DNA have been reported.[11]

We report here on the interaction of tricationic water-soluble *meso*-tri(*N*-methylpyridyl) corrole (**TMPC**) and its germanium(IV) derivative, **GeTMPC** (Chart 1) with *ss* and *ds* poly(rA) and poly(rC) and calf thymus DNA. The choice of the germanium derivative originates from its peculiar property

Received: March 6, 2013
Published: May 21, 2013

   dx.doi.org/10.1021/ja4023539 | *J. Am. Chem. Soc.* 2013, 135, 8632−8638

Chart 1. Structure of 5,10,15-Tri(*N*-methylpiridyl) Corrole and Germanium Derivative

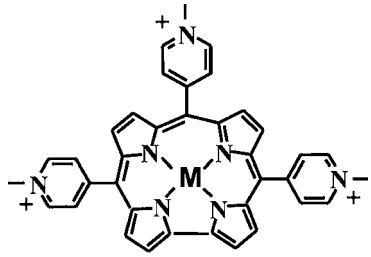

of having an axial hydroxo group that is not tightly bound to the central metal and can be easily displaced by ligand substitution[12] or allow for the formation of μ-oxo dimers.[13]

Owing to the structural similarities between porphyrins and corroles, we assume that the binding modes of these molecules are very much similar, namely, intercalation,[14a,b] external binding, and aggregation, and are characterized from the same spectroscopic features (see Figure 1).[14]

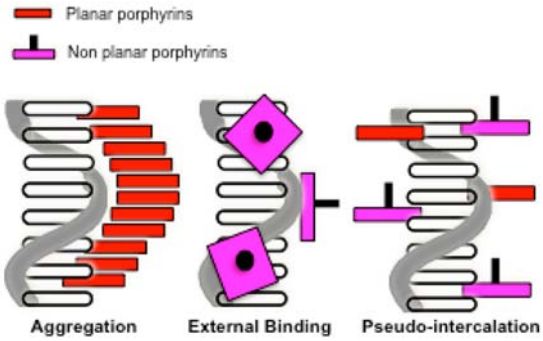

Figure 1. Porphyrins/single-helix polynucleotides binding mode.

To evaluate corrole/DNA interactions, we have employed four different spectroscopic techniques, namely, absorption, circular dichroism (CD), fluorescence, and resonance light scattering (RLS). This choice originates from the need of thoroughly characterize the title interactions by exploiting the different and specific information coming from each technique. As will be shown hereafter, this approach turned out to be decisive to distinguish between different binding modes, and before discussing the experimental results, we thought helpful to give a quick overview of the usefulness of the various techniques in this specific field.

Absorption gives fast, intuitive but not always detailed information about the type of interaction. Aggregation and intercalation leads to hypochromicity of the Soret band (more intense for aggregation than for intercalation) and, normally, to a red shit of about 10 nm or more.[14]

CD measurements are, in general, more specific because interactions of these macrocycles with polynucleotides (which are conformationally chiral) induce a dichroic band (ICD) in the absorption region of the achiral ligands (corroles, in this case). The shape and intensity of corrole ICD is diagnostic of the type of interaction (e.g., external binding, intercalation, or aggregation), and it is sketched in Figure 1.

Fluorescence can help in discriminating between external binding and intercalation. In fact, the first binding mode might lead to increase the emission intensity, owing to the decrease of vibrational freedom, whereas the second type normally leads to emission quenching.[7a] Also, aggregation leads to extensive quenching of the macrocycle emission.

The latter dichotomy can be solved by RLS, which is very specific in detecting aggregation.[15] Therefore, summarizing, we expect: (i) for intercalation: a red shift of the Soret band and some hypochromicity, a negative ICD, some fluorescence quenching, and no RLS signal; (ii) for external binding: a red shift of the Soret band, a hypochromic effect smaller than that observed for intercalation, a positive ICD or no signal, no variations of fluorescence (or a small increase in the intensity owing to the lost of vibrational freedom degrees), and no RLS signal; and (iii) for aggregation: a red or blue shift (for J- and H-aggregates, respectively) and broadening of the Soret band accompanied by extended hypochromicity, a bisignate ICD, heavy fluorescence quenching, and the presence of RLS signal, whose intensity is proportional to the size of the aggregate.

RESULTS AND DISCUSSION

Before discussing the interactions with calf thymus DNA, we will present the data obtained for the *ss* and *ds* homopolymers poly(rA) and poly(rC). It is known, in fact, that both the poly(rA) and poly(rC) exist as a single helix at pH 7 and can form a double helix at pH values close to the protonation of N1 (pK_a < 4) and N3 ($pK_a \approx 4.5$), respectively.[16]

The absorption spectrum of **TMPC** shows a main absorption (Soret band) at 492 nm and two smaller bands at 359 and 667 nm, respectively. In the presence of *ss* poly(rA) (pH 7, cacodylate buffer 1 mM), the absorption of **TMPC** shows hypochromic effects (H = 13%) and is blue-shifted by 3 nm (bottom part of the inset of Figure 2, red curve). These changes

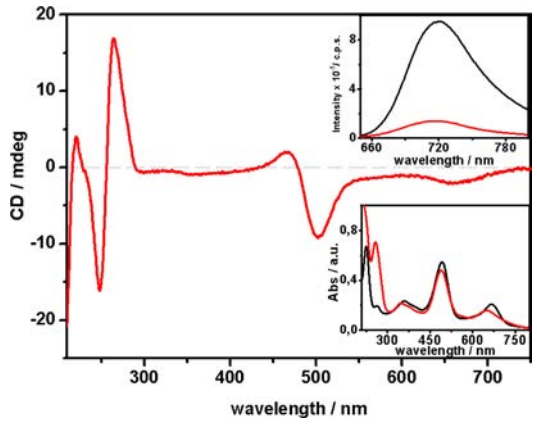

Figure 2. CD spectra of **TMPC** 10 μM in the presence of poly(rA) 50 μM in cacodylate buffer 1 mM pH = 7. Insets show fluorescence and UV spectra of **TMPC** 10 μM in absence (black curves) and in the presence (red curves) of poly(rA).

fit with both intercalation and aggregation. Yet, analysis of the CD spectrum reveals the appearance of a negative exciton split ICD, with a negative band at 510 nm and a positive one at 460 nm (Figure 2 red curve), which strongly supports corroles self-aggregation onto the polynucleotide surface.

The latter hypothesis is confirmed by the observed quenching of **TMPC** fluorescence in presence of *ss* poly(rA), which is a strong sign of direct communication between the corrole's molecules (top part of the inset of Figure 2, red curve).

dx.doi.org/10.1021/ja4023539 | J. Am. Chem. Soc. 2013, 135, 8632−8638

RLS data do not evidence strong scattering features, but only a small signal in the absorption region of **TMPC** (Figure 3 red curve) that indicates the formation of small aggregates.

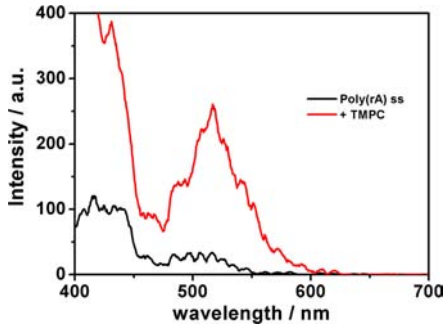

Figure 3. RLS spectra of poly(rA) 50 μM (in cacodylate buffer 1 mM pH = 7), before (black curve) and after addition of **TMPC** 10 μM (red curve).

Interactions of **TMPC** with *ss* poly(rC) are accompanied by spectroscopic changes very similar to those observed for the previous system. The main difference is observed in the absorption spectra. Also in this case, in fact, the Soret band experiences hypochromicity (H = 36%) by interactions with *ss* poly(rC), but now the Soret band is red-shifted by 25 nm (inset Figure 4 red curve). The CD spectrum shows a bisignate

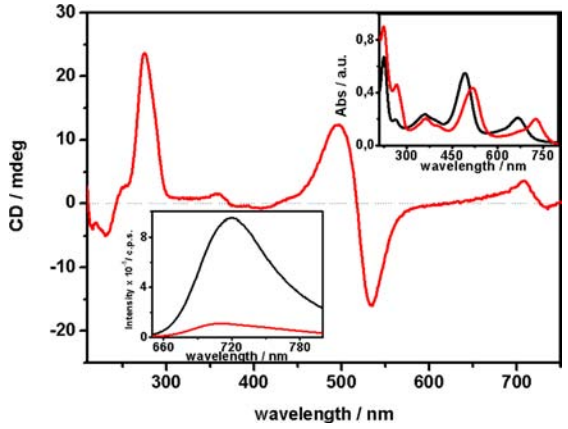

Figure 4. CD spectra of **TMPC** 10 μM in presence of the poly(rC) 50 μM in cacodylate buffer 1 mM pH = 7. Insets shows fluorescence and UV spectra of **TMPC** 10 μM in absence (black curves) and in the presence (red curves) of the poly(rC).

induced signal (a negative band centered at 530 nm and a positive band at 500 nm, red curve Figure 4) and the RLS profile a small signal, indicative of the formation of small aggregates (Figure 5 red curve). All these changes are just more pronounced than those observed for the interactions of **TMPC** with *ss* poly(rA) and are in agreement with corroles aggregation, which is also confirmed by **TMPC** fluorescence quenching (inset Figure 4 red curve).

The different shift observed in the UV spectra for the complexation of **TMPC** with poly(rA) or poly(rC) deserves a specific discussion. According to Kasha's rule,[17] the blue- and red-shifts of the chromophore absorption, upon aggregation, are related to H- (face to face) and J-type (edge to edge) disposition of the monomers in the assemblies, respectively. So, it looks like that *ss* poly(rA) promotes H-type stacking, while

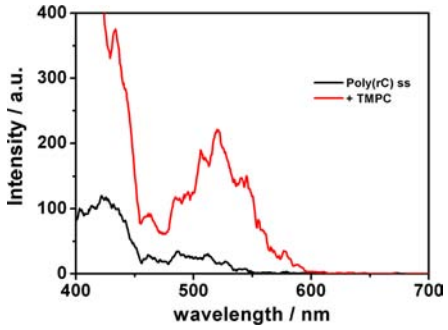

Figure 5. RLS spectra of poly(rC) 50 μM (in cacodylate buffer 1 mM pH = 7), before (black curve) and after addition of **TMPC** 10 μM (red curve).

poly(rC) induces J-type aggregation. This difference is, very likely, related to the structural differences between the two polymers, as the greater extension of purine π system and/or the smaller distance between adjacent phosphate groups for the poly(rA) polymers (its axial rise (2.7 Å) per residue is smaller than that of poly(rC) (3.2 Å)).[16]

In order to investigate the influence of the steric hindrance on the interactions of corroles with *ss* polynucleotides, we have also studied the behavior of the germanium(IV) derivative of the title corrole (**GeTMPC**). As anticipated, this metallo derivative is penta-coordinated for the presence of an axial −OH group,[12] and this should hinder both complete intercalation and self-aggregation.

CD, fluorescence, and RLS features of **GeTMPC** in the presence of *ss* poly(rA) clearly indicate some electronic communication between two or more corroles. In particular, the observation of a negative splitted ICD signal (+440 nm, −475 nm, Figure 6 black curve), fluorescence quenching

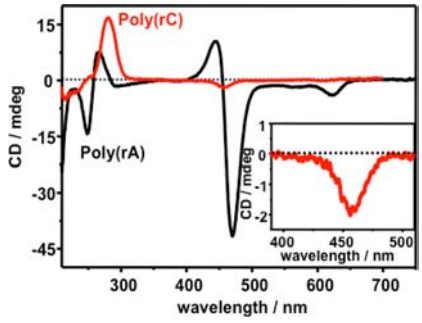

Figure 6. CD spectra of **GeTMPC** 10 μM in cacodylate buffer 1 mM pH = 7 in presence of the poly(rA) 50 μM (black curve) and poly(rC) 50 μM (red curve). Inset: zoom of **GeTMPC** signal in presence of the poly(rC) single helix.

(Figure 7, black curve), and small hypocromic (10%) effects of the absorption Soret band suggest the formation of aggregates (bottom inset of Figure 7, black curve). Owing to the presence of the axial ligand, which hinders the formation of large aggregates, it would be reasonable to hypothesize the formation of dimers. On the other hand, formation of dimers of the (penta-coordinated) zinc derivative of the tetra-anionic 5,10,15,20-*meso*-tetrakis(4-sulphonatephenyl)porphine onto polylysine has been already reported.[18] This hypothesis is also supported by the facile formation of μ-oxo dimers showed by **GeTMPC**, depending on the solution conditions.[13] Yet, according to the RLS theory[19] the threshold assembly size to

dx.doi.org/10.1021/ja4023539 | J. Am. Chem. Soc. 2013, 135, 8632−8638

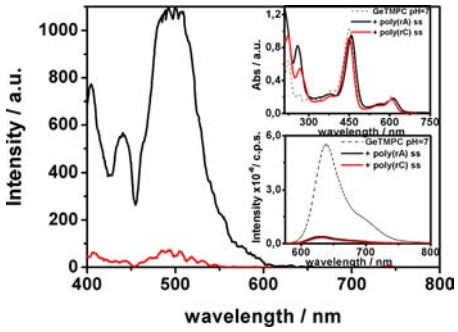

Figure 7. RLS, fluorescence (inset), and UV (inset) spectra of **GeTMPC** 10 μM in cacodylate buffer 1 mM pH = 7 in presence of the poly(rA) 50 μM (black curve) and poly(rC) 50 μM (red curve). Dotted lines refer to the spectra of **GeTMPC** 10 μM in cacodylate buffer 1 mM pH = 7.

observe an RLS signal is close to 10 monomers. We can, then, suppose that various μ-oxo dimers are in electronic contacts along the surface of the nucleotide allowing (using the two "clean" faces) for the formation of large self-assemblies.

In the presence of the *ss* poly(rC), owing to the larger distance between the basis (3.2 Å in polyC, 2.7 Å in polyA), pseudointercalation of **GeTMPC** is predominant, as shown by: (i) a small negative CD signal at 460 nm; (ii) hypocromicity (H = 12%) of the absorption Soret band; (iii) fluorescence quenching; and (iv) the absence of RLS band (Figures 6 and 7 red curve). Noteworthy, these data underline the role of the axial hindrance to foster the selectivity of porphyrinoids systems that can be exploited to specifically address corroles on given targets.

Finally, we decided to investigate the interactions of both naked **TMPC** and its germanium derivative with the double helices formed from the two investigated homopolymers. As already discussed, both poly(rA) and poly(rC) can adopt double-helix structures in aqueous solution. At pH below 4, adenosine bases are protonated and poly(rA) transforms into a double helix with a parallel strand, stabilized by four H-bounds per base pair.[20] As concerns poly(rC), at pH values around the pK_a of cytosine (4.5), a double helix with parallel chains and hemiprotonated base pair CH$^+$−C has been proposed.[21]

Differently from what observed with *ss* poly(rA), in the presence of *ds* (pH 3 by citrate buffer 1 mM), a small negative ICD signal appears, in the **TMPC** Soret region (Figure 8), but no changes in absorption and fluorescence spectra of **TMPC** in presence of the poly(rA) are observed (Figure S1 blue curves).

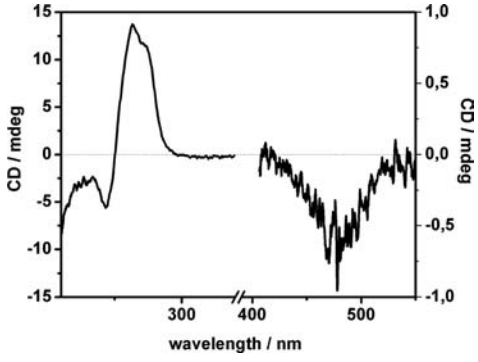

Figure 8. CD spectra of **TMPC** 10 μM in the presence of poly(rA) 50 μM in citrate buffer 1 mM pH = 3.

At pH 3, both the macrocycles and the bases of poly(rA) are positively charged. In particular, the positive charge of **TMPC** (pK_a = 4.5) increases by one unit, owing to the protonation of the central nitrogen, and because of the protonated adenines and partially protonated phosphate groups, also poly(rA) *ds* has a lower negative potential with respect with the *ss* parent. This charge distribution causes an electrostatic repulsion that hinders interaction between corrole and *ds*, allowing just a weak pseudointercalation, as indicated by CD spectroscopy.

The *ds* poly(rC) was induced in citrate buffer 1 mM at pH 3.5.[22] Following the addition of 10 μM of **TMPC**, an ICD signal is observed in the absorption region of corrole. This signal displays a trisignate shape (a negative small band at 480 nm sided by two positive bands at about 400 and 500 nm, respectively; Figure 9), which could be assigned to vibrational

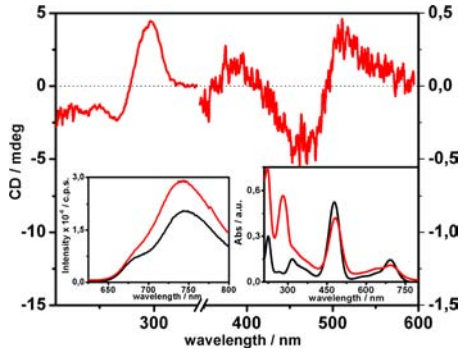

Figure 9. CD spectra of **TMPC** 10 μM in presence of the poly(rC) 50 μM in citrate buffer 1 mM pH = 3.5. Insets shows fluorescence and UV spectra of **TMPC** 10 μM in absence (black curves) and in the presence (red curves) of the poly(rC).

modes of electronically coupled corroles[23] or to the contemporary occurrence of different binding modes. We are more prone to consider the complexity of the ICD signal as arising from a multibinding mode of corroles, in particular, from a negative band, suggesting intercalation of the **TMPC** in the presence of the poly(rC) *ds*, and one (large) positive ICD indicating external binding. So, the trisignate shape should result from the "intermission" of the negative band into the positive one. This hypothesis is reinforced by UV and fluorescence spectra. The Soret band is broadened and red-shifted ($\Delta\lambda$ 2 nm), with 20% of hypocromic effect (typical intercalation sign), while an increase in the fluorescence emission indicates a decrease of free vibrational degree due to immobilization of **TMPC** on the double helix (Figure 9 red curve).

GeTMPC shows the same spectroscopic signal in the presence of both polynucleotides in *ds*: (i) a small negative CD signal (~450 nm) (Figure 10); (ii) no changes of the absorption Soret band (Figures S2 and S3); and (iii) a small quenching of fluorescence (Figure S3). In this case we hypothesize that **GeTMPC** is only partially intercalated (pseudointercalated) because these spectroscopic signs indicate a weak interaction of Germanium corrole with both *ds* poly(rA) and poly(rC), not involving the whole macrocyclic ring.

We also tested the naked **TMPC** in the presence of calf thymus DNA. The addition of increasing concentration of corroles to a solution of DNA with 10 mM of NaCl produces strong distortions of the calf thymus conformation as shown in Figure 11. In the CD spectra, after addition of **TMPC** to DNA solution, a small negative ICD signal appears at about 490 nm,

dx.doi.org/10.1021/ja4023539 | J. Am. Chem. Soc. 2013, 135, 8632−8638

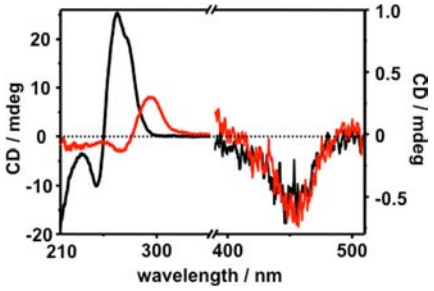

Figure 10. CD spectra of **GeTMPC** 10 μM in citrate buffer 1 mM pH = 3.5 in presence of the poly(rA) 50 μM (black curve) and poly(rC) 50 μM (red curve).

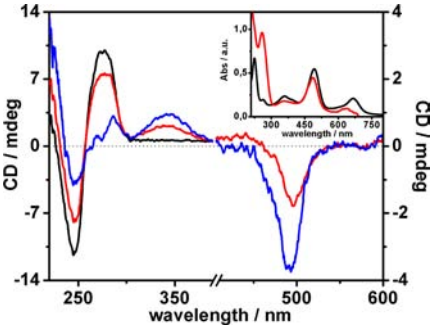

Figure 11. CD spectra of calf thymus DNA 50 μM in cacodylate buffer 1 mM pH = 7 and NaCl 10 mM in the absence (black curve) and in the presence of **TMPC** 10 μM (red curve) and 30 μM (blue curve). Insets shows UV spectra of **TMPC** 10 μM in the absence (black curves) and in the presence (red curves) of calf thymus DNA.

and a positive cotton effect is observed at 350 nm, with drastic reduction of the DNA signal below 300 nm. In the UV absorption spectra, hypochromic effect (H = 13%) and blue shift ($\Delta\lambda$ 5 nm) are observed (inset Figure 11). This spectroscopic evidence prompts the intercalation of **TMPC** between the DNA bases causing distortion in the DNA conformation.

In order to confirm **TMPC** intercalation, we carried out melting experiments (Figure S4); intercalation is, in fact, generally accompanied by an increase of the *ds* melting temperature (T_m).[13a] Indeed, the T_m of CT-DNA increases upon interaction with **TMPC** (at low corrole/DNA ratio 0.1) by about 4 °C in buffer solution at pH = 7. Increasing the concentration of TMPC causes a distortion in the DNA conformation and a consequent destabilization of the double helix to occur. In fact, the intensity of the spectrum recorder at T = 100 °C of the only CT-DNA and that at 25 °C of the DNA-**TMPC** complex at high corrole load is very similar (Figure S5).

On the contrary, the interaction between **GeTMPC** and CT-DNA seems to lead to an external binding. As proof, a positive ICD signal is observed in the Soret absorption region, with a maximum at 455 nm (Figure 12). However, no absorption variations occur. As observed previously with TMPC, some distortion in the DNA conformation is confirmed by the strong variation observed in the CD spectrum in the UV region.

EXPERIMENTAL SECTION

General. Silica gel 60 (70−230 mesh, Sigma Aldrich) or neutral alumina oxide (Grade III or IV, Merck) was used for column chromatography. Reagents and solvents (Aldrich, Fluka) were of the highest grade available and were used without further purification. Room-temperature ^{1}H NMR spectra were recorded on a Bruker AV300 spectrometer operating at 300.13 MHz. Chemical shifts are given in ppm relative to residual solvent ($CDCl_3$ 7.26 ppm, D_2O 4.79 ppm).

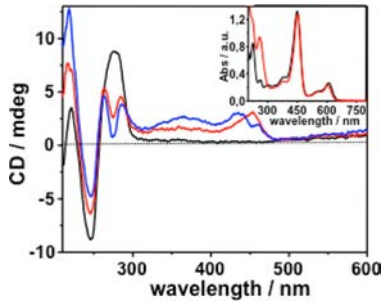

Figure 12. CD spectra of calf thymus DNA 50 μM in cacodylate buffer 1 mM pH = 7 and NaCl 10 mM in the absence (black curve) and in the presence of **GeTMPC** 10 μM (red curve) and 20 μM (blue curve). Inset shows UV spectra of **GeTMPC** 10 μM in the absence (black curves) and in the presence (red curves) of calf thymus DNA.

5,10,15-Tri(4-pyridyl) Corrole. Pyrrole (4.2 mL, 60.5 mmol) and 4-pyridinecarboxaldehyde (1.9 mL, 20.2 mmol) were dissolved in 250 mL of acetic acid. The solution was refluxed under stirring, and the course of the reaction was monitored by UV−vis measurements; after 4 h, the reaction mixture was cooled, and the solvent removed under reduced pressure. The residue was dissolved in $CHCl_3$ and purified by neutral alumina column (Grade III) eluted with $CHCl_3$. The fractions containing the title corrole were collected, the solvent was reduced to a small volume, and the mixture further purified by neutral alumina column (Grade IV) eluted with CH_2Cl_2. A green band was collected, the solvent removed under reduced pressure, and the residue crystallized by CH_2Cl_2/ hexane, yielding 320 mg of the title corrole (Yield 9%). UV−vis (CH_2Cl_2), λ_{max} (log ε): 417 (5.08), 576 (4.36), 616 (4.26), 651 (4.24). ^{1}H NMR ($CDCl_3$) δ −1.76 (br s, 3H), 8.16 (d, 2H, J = 5 Hz), 8.30 (d, 4H, J = 5 Hz), 8.63 (d, 2H, J = 5 Hz), 8.68 (d, 2H, J = 5 Hz), 8.95 (d, 2H, J = 5 Hz), 9.02 (d, 2H, J = 5 Hz), 9.06 (d, 4H, J = 5 Hz), 9.12 (d, 2H, J = 5 Hz). LRMS (FAB): m/z 530 (M^+). Anal. calcd for $C_{34}H_{23}N_7$: C, 77.11; H, 4.38; N, 18.51. Found: C, 76.92; H, 4.52; N, 18.19.

[5,10,15-Tri(4-pyridyl) Corrole]Ge(OH). 5,10,15-Tri(4-pyridyl) corrole (70 mg, 0.132 mmol) was dissolved in dry DMF (10 mL), $GeCl_4$ (68 μL, 0.585 mmol) was added under nitrogen, and the mixture refluxed for 1.5 h, monitoring the course of the reaction by UV−vis spectrometry. After the complex formation, the solvent was removed under vacuum, and the residue purified by column chromatography on neutral alumina (Grade III) eluted with CH_2Cl_2/CH_3OH (10:1). Fractions containing Ge-corrole were collected, the solvent removed under vacuum, and residue crystallized by CH_2Cl_2/hexane. (Yield 37 mg, 46%). UV−vis (CH_2Cl_2), λ_{max} (log ε): 414 (5.23), 521 (3.89), 560 (3.99), 586 (4.32). ^{1}H NMR ($CDCl_3$) δ −4.06 (br s, axial −OH), 8.26−8:31 (m, *meso*-pyridyl, 4H), 8.97 (br d, β-pyrrole, 2H), 9.09−9.12 (m, *meso*-pyridyl + β-pyrrole, 10 H), 9.25 (br d, β-pyrrole, 2H), 9.51 (br d, β-pyrrole 2H). Anal. calcd for $C_{34}H_{21}GeN_7O$: C, 66.27; H, 3.43; N, 15.91. Found: C, 66.31; H, 3.49; N, 15.86.

[5,10,15-Tri(*N*-methyl-4-pyridyl) Corrole]Ge(OH), Iodide Salt. [5,10,15-Tri(4-pyridyl) corrole]Ge(OH) (40 mg, 0.065 mmol) was dissolved in dry DMF (12 mL), CH_3I (65.54 mL, 89 mmol) was added under nitrogen, and the mixture was stirred under nitrogen at room temperature in the dark for 24 h. The solvent and excess CH_3I were removed under reduced pressure. The crude product was crystallized by methanol/diethyl ether. (Yield 62 mg, 91%). UV−vis (CH_3OH), λ_{max} (log ε): 379 (4.03), 455 (4.99), 560 (3.62), 615 (3.88). ^{1}H NMR (D_2O): 4.65 (s, N^+CH_3 9H), 8.78−8.80 (m, *meso*-pyridyl + β-pyrrole, 4H), 8.87−8.92 (m, *meso*-pyridyl + β-pyrrole, 4H), 9.12 (d, β-pyrrole, 2H, J = 4.24 Hz), 9.17−9.22 (m, *meso*-pyridyl, 8H),

dx.doi.org/10.1021/ja4023539 | J. Am. Chem. Soc. 2013, 135, 8632−8638

Table 1. Spectral Properties of Complexes of TMPC and Ge(IV) Derivative with Poly(rA) and Poly(rC) *ss* and *ds*

		TMPC				GeTMPC			
RNA type		Abs	CD	Fluo	binding mode	Abs	CD	Fluo	binding mode
poly(rA)	*ss*	hypo 13% blue shift Δλ 3 nm	+ 460 nm - 510 nm	quenching	H-aggregate	hypo 10% red shift Δλ 8 nm	+440 nm −475 nm	quenching	dimerization/ aggregation
	ds	–	- 470 nm	–	pseudointercalation	–	−450 nm	–	pseudointercalation
poly(rC)	ss	hypo 36% red shift Δλ 25 nm	+ 500 nm - 530 nm	quenching	J-aggregate	hypo 10%	−460 nm	quenching	pseudointercalation
	ds	hypo 20% red shift Δλ 2 nm	+ 510 nm - 480 nm + 410 nm	increase	pseudointercalation	–	−450 nm	–	pseudointercalation

9.33 (d, β-pyrrole, 2H, J = 4.76 Hz). Anal. calcd for $C_{37}H_{30}GeI_3N_7O$: C, 42.65; H, 2.90; N, 9.41. Found: C, 42.69; H, 2.87; N, 9.36.

Nucleic acid homopolymers are dissolved in cacodylate buffer 1 mM (pH = 7) to obtain single helix or in citrate buffer 1 mM (pH = 3 for poly(rA) or pH = 3.5 for poly(rC)) to obtain double helix. CD and UV measurements were carried out with a spectropolarimeter JASCO J-710 and a spectrophotometer JASCO V-530, respectively. For the fluorescence and RLS data, a fluorolog FL-11 Jobin-Yvon Horiba was used. **TMPC** was excited at λ 490 nm and **GeTMPC** at λ 450 nm; at these wavelengths, the absorbance in all experiment was very similar, thus no correction of the absorption was carried out for the fluorescence spectra. All compounds were dissolved in ultrapure water obtained from Elga Purelab Flex system by Veolia.

CONCLUSION

A combined use of CD, UV−vis absorption, fluorescence, and RLS spectroscopy has demonstrated that **TMPC** is a promising probe for *ss* nucleic acid because it is able to discriminate between *ss* and *ds* conformations of nucleic acid homopolymers (Table 1). Furthermore, we have shown that this macrocycle is an intercalating agent that, at high doses, destabilizes the double helix of DNA.

Finally, **GeTMPC** derivative can distinguish between *ss* polyadenilic and polycytosine acids, forming μ-oxo dimers in the presence of poly(rA) *ss* and weakly intercalating in presence of the poly(rC) *ss* (Table 1).

ASSOCIATED CONTENT

Supporting Information

Absorption and fluorescence spectra of **TMPC** in the presence of *ds* poly(rA); absorption and fluorescence spectra of **GeTMPC** in the presence of *ds* poly(rA) and *ds* poly(rC). This material is available free of charge via the Internet at http://pubs.acs.org.

AUTHOR INFORMATION

Corresponding Author

rpurrello@unict.it; roberto.paolesse@uniroma2.it

Notes

The authors declare no competing financial interest.

ACKNOWLEDGMENTS

This work was financially supported by MIUR−PRIN 2009A5Y3N9 and FIRB 2012 RBFR12WB3W.

REFERENCES

(1) (a) Edmonds, M.; Winter, M. A. *Prog. Nucleic Acid Res. Mol. Biol.* **1976**, *17*, 149−179. (b) Ahlquist, P.; Kaesberg, P. *Nucleic Acids Res.* **1979**, *7* (5), 1195−1204.

(2) Habano, W.; Sugai, T.; Yoshida, T.; Nakamura, S. *Int. J. Cancer* **1998**, *5*, 695−696.

(3) Schwartz, S., Jr.; Alazzouzi, H.; Perucho, M. *Genes, Chromosomes Cancer* **2006**, *45* (8), 770−780.

(4) (a) Tanaka, K.; Okamoto, A. *Bioorg. Med. Chem.* **2008**, *16*, 400−404. (b) Duke, M.; Palmenberg, A. C. *J. Virol.* **1989**, *63*, 1822−1826.

(5) (a) Pasternack, R. F.; Brigandi, R. A.; Abrams, M. J.; Williams, A. P.; Gibbs, E. J. *Inorg. Chem.* **1990**, *29*, 4483−4486. (b) Bustamante, C.; Guerrieri, S.; Pasternack, R. F.; Purrello, R.; Rizzarelli, E. *Biopolymers* **1994**, *34*, 1099−1104. (c) Pastenack, R. F.; Gurrieri, S.; Lauceri, R.; Purrello, R. *Inorg. Chim. Acta* **1996**, *246*, 7−12.

(6) Belmont, P.; Constant, J.-F.; Demeunynck, M. *Chem. Soc. Rev.* **2001**, *30*, 70−81.

(7) (a) Balaz, M.; De Napoli, M.; Holmes, A. E.; Mammana, A.; Nakanishi, K.; Berova, N.; Purrello, R. *Angew. Chem., Int. Ed.* **2005**, *44*, 4006−4009. (b) D'Urso, A.; Holmes, A. E.; Berova, N.; Balaz, M.; Purrello, R. *Chem. Asian J.* **2011**, *6*, 3104−3109. (c) Meunier, B.; Robert, A.; Pratviel, G.; Bernadou, J. In *The Porphyrin Handbook*; Kadish, K. M., Smith, K. M., Guilard, R., Eds.; Academic Press: New York, 2000, *4*, 164−171.

(8) (a) Dougherty, T. J.; Gomer, C. J.; Henderson, B. W.; Jori, G. *J. Natl. Cancer Inst.* **1998**, *90*, 889−905. (b) Pandey, R. K. Zheng, G. In *The porphyrin Handbook*; Kadish, K. M., Smith, K. M., Guilard, R., Eds.; Academic Press: Boston, 2000, *6*, 157−230.

(9) (a) Aviezer, D.; Cotton, S.; David, M.; Segev, A.; Khaselev, N.; Galili, N.; Gross, Z.; Yayon, A. *Cancer Res.* **2000**, *60*, 2973−2980. (b) Okun, Z.; Kupershmidt, L.; Amit, T.; Mandel, S.; Bar-Am, O.; Youdim, M. B. H.; Gross, Z. *Chem. Biol.* **2009**, *11*, 910−914. (c) Ma, H.; Zhang, M.; Zhang, D.; Huang, R.; Zhao, Y.; Yang, H.; Liu, Y.; Weng, X.; Zhou, Y.; Deng, M.; Xu, L.; Zhou, X. *Chem. Asian J.* **2010**, *5*, 114−122. (d) Agadjanian, H.; Ma, J.; Rentsendorj, A.; Valluripalli, V.; Hwang, J. Y.; Mahammed, A.; Farkas, D. L.; Gray, H. B.; Gross, Z.; Medina-Kauwe, L. K. *Proc. Natl. Acad. Sci. U.S.A.* **2009**, *106* (15), 6105−6110.

(10) (a) Paolesse, R.; Nardis, S.; Sagone, F.; Khoury, R. G. J. *Org. Chem.* **2001**, *66*, 550−556. (b) Gershman, Z.; Goldberg, I.; Gross, Z. *Angew. Chem.* **2007**, *119*, 4398−4402; *Angew. Chem., Int. Ed.* **2007**, *46*, 4320−4324. (c) Lu, J.; Liu, H. Y.; Shi, L.; Wang, X. L.; Ying, X.; Zhang, L.; Ji, L. N.; Zang, L. Q.; Chang, C. K. *Chin. Chem. Lett.* **2011**, *22*, 101−104. (d) Fu, B.; Huang, J.; Ren, L.; Weng, X.; Zhou, Y.; Du, Y.; Wu, X.; Zhou, X.; Yang, G. *Chem. Commun.* **2007**, 3264−3266. (e) Fu, B. Q.; Zhang, D.; Weng, X. C.; Zhang, M.; Ma, H.; Ma, Y. Z.; Zhou, X. *Chem.—Eur. J.* **2008**, *14*, 9431−9441.

(11) (a) D'Urso, A.; Mammana, A.; Balaz, M.; Holmes, A. E.; Berova, N.; Lauceri, R.; Purrello, R. *J. Am. Chem. Soc.* **2009**, *131*, 2046−2047. (b) D'Urso, A.; Kyu Choi, J.; Shabbir-Hussain, M.; Ngwa, F. N.; Lambousis, M. I.; Purrello, R.; Balaz, M. *Biochem. Biophys. Res. Commun.* **2010**, *397*, 329−332.

(12) (a) Paolesse, R.; Licoccia, S.; Boschi, T. *Inorg. Chim. Acta* **1990**, *178*, 9−12. (b) Simkhovich, L.; Mahammed, A.; Goldberg, I.; Gross, Z. *Chem.—Eur. J.* **2001**, *7*, 1041−1055.

(13) (a) Mastroianni, M.; Zhu, W.; Stefanelli, M.; Nardis, S.; Fronczek, F. R.; Smith, K. M.; Ou, Z.; Kadish, K. M.; Paolesse, R.

Inorg. Chem. **2008**, *47*, 11680−11687. (b) Nardis, S.; Mandoj, F.; Paolesse, R.; Fronczek, F. R.; Smith, K. M.; Prodi, L.; Montalti, M.; Battistini, G. *Eur. J. Inorg. Chem.* **2007**, 2345−2352.
(14) (a) Fiel, R. J.; Howard, J. C.; Mark, E. H.; Dattagupta, N. *Nucleic Acids Res.* **1979**, *6*, 3093−3118. (b) Banville, D. L.; Marzilli, L. G.; Wilson, D. W. *Biochem. Biophys. Res. Commun.* **1983**, *113*, 148. (c) Fiel, R. J. *J. Mol. Struct.* **1989**, *6*, 1259−1274. (d) Pasternack, R. F.; Gibbs, E. J.; Villafranca, J. J. *Biochemistry* **1983**, *22*, 2406−2414. (e) Pasternack, R. F. *Chirality* **2003**, *15*, 329−332.
(15) (a) Pasternack, R. F.; Collings, P. J. *Science* **1995**, *269*, 935−939. (b) Pasternak, R. F.; Bustamante, C.; Collings, P. J.; Giannetto, A.; Gibbs, E. J. *J. Am. Chem. Soc.* **1993**, *115*, 5393−5399.
(16) Saenger, W. *Principles of Nucleic Acid Structure*; Springer-Verlag: New York, 1988.
(17) Kasha, M.; Rawls, H. R.; El Bayoumi, M. A. *Pure Appl. Chem.* **1965**, *11*, 371−392.
(18) Purrello, R.; Bellacchio, E.; Gurrieri, S.; Lauceri, R.; Raudino, A.; Monsù Scolaro, L.; Santoro, A. M. *J. Phys. Chem. B* **1998**, *102*, 8852−8857.
(19) Parkash, J.; Robblee, J. H.; Agnew, J.; Gibbs, E.; Collings, P.; Pasternack, R. F.; de Paula, J. C. *Biophys. J.* **1999**, *74*, 2089−2099.
(20) (a) Evans, F. E.; Sarma, R. H. *Nature* **1976**, *263*, 567−572. (b) Prescott, B.; Gamache, R.; Livramento, J.; Thomas, G. J. *Biopolymers* **1974**, *13*, 1821−1845. (c) Brahms, J.; Michelson, A. M.; Van Holde, K. E. *J. Mol. Biol.* **1966**, *15*, 467−488.
(21) Borah, B.; Wood, J. L. *J. Mol. Struct.* **1976**, *30*, 13−30.
(22) The formation of *i*-motif cannot be excluded, however the induction of tertiary structures occurs in different experimental conditions as reported in the following references: (a) Snoussi, K.; Nonin-Lecomte, S.; Leroy, J.-L. *J. Mol. Biol.* **2001**, *309* (1), 139−153. (b) Stephenson, A. W. I.; Partridge, A. C.; Filichev, V. V. *Chem.—Eur. J.* **2011**, *17*, 6227−6238. (c) Chakraborty, S.; Krishnan, Y. *Biochimie* **2008**, *90*, 1088−1095. (d) Li, T.; Ackermann, D.; Hall, A. M.; Famulok, M. *J. Am. Chem. Soc.* **2012**, *134* (7), 3508−3516 However, even if the *i*-motif was formed, the general conclusions would, in principle, be the same.
(23) Piscitelli, G.; Gabriel, S.; Wang, Y.; Fleischhauer, J.; Woody, R. W.; Berova, N. *J. Am. Chem. Soc.* **2003**, *125*, 7613−28.